

## Control of the Dephasing of Image-Potential States by CO Adsorption on Cu(100)

Ch. Reuß, I. L. Shumay, U. Thomann, M. Kutschera, M. Weinelt, and Th. Fauster

*Lehrstuhl für Festkörperphysik, Universität Erlangen-Nürnberg, Staudtstraße 7, D-91054 Erlangen, Germany*

U. Höfer

*Max-Planck-Institut für Quantenoptik, D-85740 Garching, Germany and Physik Department, Technische Universität München, D-85747 Garching, Germany*

(Received 2 September 1998)

The dynamical behavior of image-potential states has been studied with two-photon photoemission for CO on Cu(100). Pure dephasing is observed as the loss of coherence in quantum beats, or derived from linewidth and lifetime measurements. A correlation to the surface order as observed by low-energy electron diffraction is also established. [S0031-9007(98)08070-3]

PACS numbers: 73.20.At, 79.60.Bm, 79.60.Dp, 79.60.Ht

The study of the dynamics of electrons at metal surfaces is important for the understanding of photon or electron-induced chemical reactions in adsorbate overlayers [1]. Recent progress has been advanced by the generation of ultrashort laser pulses [2]. Two-photon photoelectron spectroscopy of image-potential states [3] permits the detailed study of the electron dynamics in the energy as well as in the time domain [4]. The results show a complex behavior of the measured decay time as a function of the energy analyzer detuning from the main peak and of the linewidth as a function of time delay between the two photon pulses [5]. A consistent description can be reached by the use of the Liouville-von Neumann equations [6,7]. The main parameters entering this picture are the true lifetime  $\tau$  of the image-potential state as well as the pure dephasing times  $T^*$  of the initial and intermediate states. The lifetime describes the decay of the population by inelastic scattering events and is measured in time-resolved experiments. Additional pure dephasing can be attributed to quasielastic scattering processes which do not change the population of the image-potential state but destroy the coherence between the involved states. This increases the measured energy width  $\Gamma$  compared to the value expected from the lifetime  $\hbar/\tau$ . These processes are indicated in Fig. 1 together with the excitation scheme of two-photon photoemission.

The true lifetime is understood fairly well theoretically by the decay of the image-state electron [8,9]. The results are closely related to the properties of hot electrons, because the decay of the image-potential states occurs mainly into metal bulk states. Using temperature-dependent measurements the quasielastic scattering by phonons could be identified and the results indicate bulklike values weighted by the probability of finding the electron inside the metal [7]. In this Letter we address surface-specific scattering processes induced by defects on the surface. As a model system we chose the adsorption of CO on Cu(100). This system shows a  $c(2 \times 2)$  phase at half a monolayer (ML) coverage and a  $c(7\sqrt{2} \times \sqrt{2})R45^\circ$  compression phase at

the saturation coverage of 0.57 ML [10]. For the clean and CO-covered Cu(100) surface the vacuum level is located close to the center of the band gap of the projected bulk band structure and a series of image-potential states can be observed [3,4].

In the two-photon photoemission experiments we used the frequency-tripled radiation from a Ti:sapphire laser as pump pulse at photon energy  $3h\nu$  and the fundamental radiation ( $h\nu$ ) as probe pulse (see Fig. 1). The pulse widths

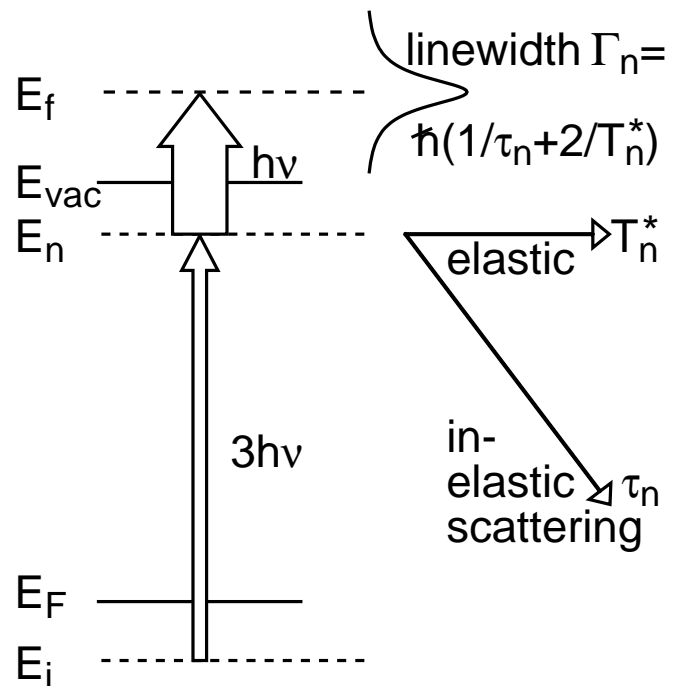


FIG. 1. Schematic representation of the bichromatic two-photon photoemission process using the frequency-tripled light  $3h\nu$  for exciting an electron from the occupied states  $E_i$  below the Fermi energy  $E_F$  and the fundamental wave  $h\nu$  for lifting the electron above the vacuum level  $E_{vac}$ . Elastic and inelastic processes contribute to the intrinsic linewidth  $\Gamma_n$  at the final state energy  $E_f$ , whereas the population in the intermediate state  $E_n$  decays with the lifetime  $\tau_n$ .

were 75 and 45 fs, respectively. The electrons emitted normal to the surface were detected after a hemispherical energy analyzer with an energy and momentum resolution of  $\sim 40$  meV and  $0.005 \text{ \AA}^{-1}$ , respectively [3]. The Cu(100) sample was cleaned and prepared by standard techniques. The adsorption of CO at 90 K was monitored by low-energy electron diffraction (LEED) avoiding long exposures to the electron beam (90 eV) by translating the sample and acquiring the full screen by a video system [11]. For a quantitative analysis the LEED spots were fitted in two dimensions by Lorentzians convoluted with Gaussian functions.

The determination of short lifetimes by pump-probe techniques depends critically on the precise knowledge of the cross correlation between pump and probe pulses. We used the occupied surface state of a Cu(111) sample mounted on the same sample holder as a reference [5]. Alternatively, the fast decaying part of the excitation of the higher image-potential states can be used [4]. For the accurate determination of the linewidth of image-potential states the contribution from the direct two-photon ionization process has to be excluded [5,12]. Therefore, the linewidth was extracted from spectra taken at time delays of 100–200 fs after the maximum overlap of the pump and probe pulses. The lifetime and intrinsic linewidth were determined by fitting procedures taking into account the experimental time and energy resolution, respectively [4,13].

The dephasing of the wave functions can be observed directly with two-photon photoemission in the time evolution of coherently excited states undisturbed by inhomogeneous broadening [4]. Such data are shown in Fig. 2 where the coherent superposition of the  $n = 3$  and  $n = 4$  image-potential states leads to oscillations with a period of  $117 \pm 2$  fs superimposed on an exponential decay representing predominantly the lifetime of the  $n = 3$  state of  $300 \pm 15$  fs. The decay of the oscillations for the clean surface occurs with a time constant of  $280 \pm 30$  fs. This value drastically decreases to  $60 \pm 10$  ( $40 \pm 10$ ) fs upon adsorption of 0.04 (0.08) ML of CO, whereas the oscillation period and lifetime  $\tau$  remain almost constant. The wave functions can be described by  $\psi_n = C_n(t)e^{iE_n t/\hbar}$  with time-dependent coefficients  $C_n(t) = c_n e^{-t/2\tau_n}$ . A coherent excitation of the  $n = 3$  and  $n = 4$  states leads to an oscillation with a period of  $\hbar/(E_3 - E_4)$  damped with a time constant of  $(1/2\tau_3 + 1/2\tau_4 + 1/T_d)^{-1}$ . The last term  $1/T_d = 1/T_3^* + 1/T_4^*$  allows for quasielastic scattering processes which destroy the phase coherence while leaving the population unchanged. The data of Fig. 2 show unambiguously that adsorption of CO on Cu(100) leads to a strong decrease of the phase coherence between the two wave functions.

The lifetime  $\tau_1$  of the  $n = 1$  image-potential state derived from time-resolved measurements is shown as a function of CO exposure by open diamonds in Fig. 3. The decay rate  $\hbar/\tau_1$  increases from 17 meV for the clean surface to  $\sim 65$  meV at an exposure of  $4 \text{ L} = 4 \times 10^{-6} \text{ Torr sec}$  which also represents the final value at

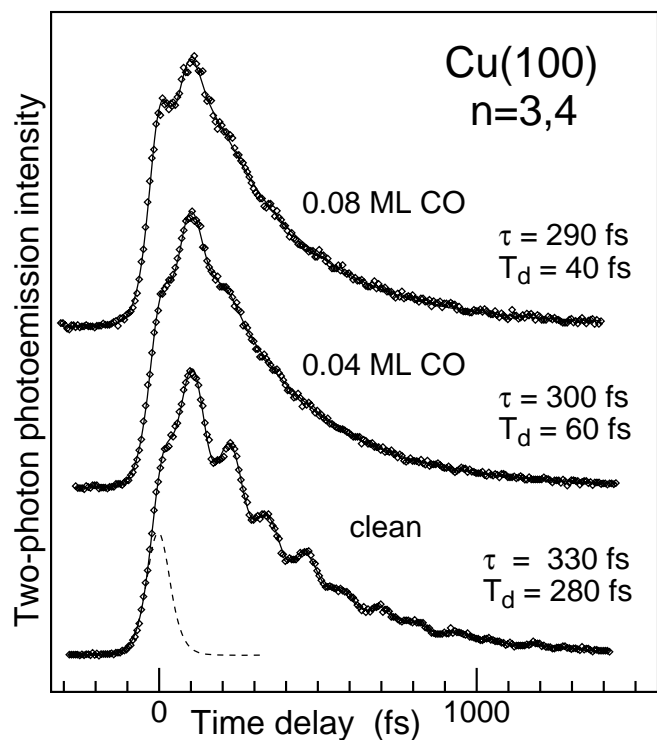


FIG. 2. Quantum beats from the coherently excited  $n = 3$  and 4 image-potential states on Cu(100). The oscillations decay rapidly ( $T_d$ ) upon CO adsorption, whereas the exponential decay representing the lifetime  $\tau \approx \tau_3$  remains almost unchanged. The dashed line shows the cross correlation between pump and probe pulse.

high coverages. Two processes contribute to the increase. (i) Additional channels for decay of the image-potential state are offered by the CO related unoccupied states around 2.5 and 3.8 eV above  $E_F$  [10]. This process would be proportional to the number of adsorbed CO molecules, i.e., the coverage. (ii) The image-state electrons can be scattered elastically by the reciprocal lattice vectors of the CO overlayer. This brings them from the Brillouin zone center at  $\bar{\Gamma}$  to the region around the zone boundary of the clean surface at  $\bar{M}$ . In this region there exists no band gap in the projected bulk band structure and the electron can escape into the bulk. This latter process should contribute efficiently at exposures above 2 L where the LEED superstructures are visible (see Fig. 3). The data for the decay rate for exposures above 2 L are indeed above the dashed line in Fig. 3 indicating the linear increase for lower exposures. The linear increase of the decay rate is also observed for the  $n = 2$  and  $n = 3$  states starting at low exposures. We suggest that the decay into unoccupied CO related states is the dominant process at least for small coverages.

The reduction of the lifetime and the resulting increase of the decay rate must be reflected by an increase of the intrinsic linewidth. The experimental results are shown as filled squares in Fig. 3. The linewidth increases much faster and shows nonmonotonic behavior as a function of

CO exposure compared to the decay rate. The difference between the intrinsic linewidth  $\Gamma_n$  and the decay rate  $\hbar/\tau_n$  is the pure dephasing rate  $2\hbar/T_n^*$  [2]. The data are shown as filled circles in the lower panel of Fig. 3 and exhibit the structure seen in the linewidth more clearly. Particularly striking is the fact that the minima of the pure dephasing rate correspond to the ordered LEED structures observed for the clean surface and the ordered  $c(2 \times 2)$  and  $c(7\sqrt{2} \times \sqrt{2})R45^\circ$  CO structures at 0.5 and 0.57 ML coverage, respectively. A quantitative correspondence is achieved by comparing to the solid line in Fig. 3 which shows the additional width of the LEED superstructure spots relative the integral order spots. No significant difference in the spotwidth was found for the two overlayer structures in the coexistence regime.

The correlation between pure dephasing rate and LEED spotwidth supports the picture that pure dephasing is due to quasielastic scattering processes of the electron by the CO adsorbate. Characteristic for less-ordered overlayers are the increased spotwidths which correspond to scattering events with small momentum transfer. The electrons in image-potential states are influenced by the same over-

layer and the available range of momentum transfer is the same. Scattering processes with small momentum transfer ( $0.1 \text{ \AA}^{-1}$ ) lead to small energy changes (38 meV) along the free-electron-like parabola of the image-potential state. Within the experimental resolution of  $\sim 40$  meV the electron stays in the image-potential state, but the phase coherence with the exciting pulse or coherently excited states is destroyed. This shows up in an increased pure dephasing rate and the disappearance of the quantum-beat pattern, respectively.

The correspondence between the pure dephasing rate and the LEED spotwidth in the lower part of Fig. 3 correlates the inverse of time and length. These represent the time and distance between two quasielastic scattering events of the electron. The proportionality introduces a speed  $v \approx 50 \text{ meV}/(\hbar \times 0.1 \text{ \AA}^{-1}) = 0.76 \text{ \AA}/\text{fs}$ . For  $k_{\parallel} = 0$  one would expect  $v = 0$ , but the lateral localization gives a momentum  $mv = \hbar k_{\parallel}$ . A length scale of  $10 \text{ \AA}$  corresponds to a speed of  $v = 1.6 \text{ \AA}/\text{fs}$  in reasonable agreement with the value above.

Further insight into the decay and dephasing mechanisms can be gained from the dependence on the quantum number  $n$ . In Fig. 4 the decay rate for the clean Cu(100) surface is shown by open diamonds as a function of  $n$  [4,12]. The open circles represent the pure dephasing rates for the  $n = 3, 4, 5$  states obtained from the damping of the

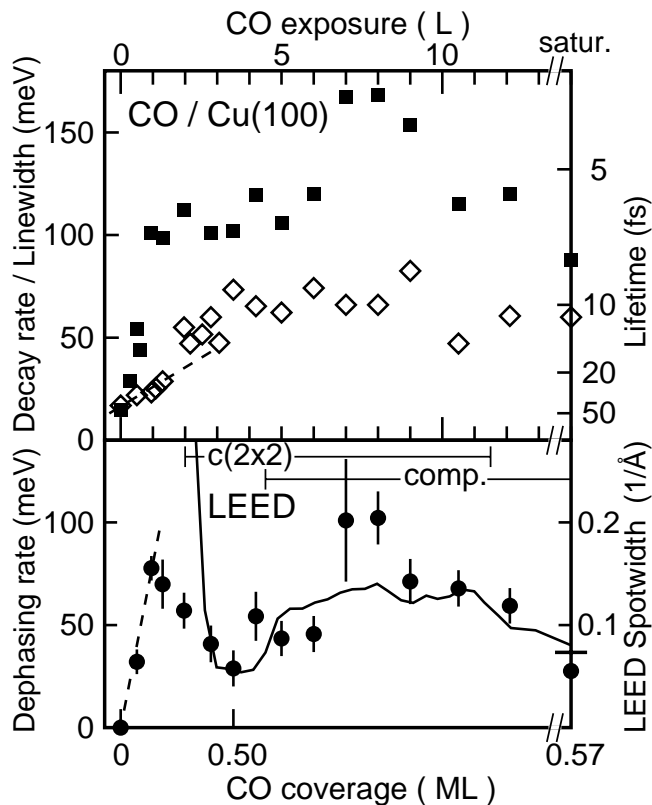


FIG. 3. Linewidth (filled squares), decay rate (open diamonds), and pure dephasing rate (filled circles) for the  $n = 1$  image-potential state as a function of CO exposure. The minima of the dephasing rate coincide with the coverages of the best ordered CO overlayers as measured by the width of the overlayer LEED spots (solid line). The existence regimes of the  $c(2 \times 2)$  and the compressed overlayer structures are indicated.

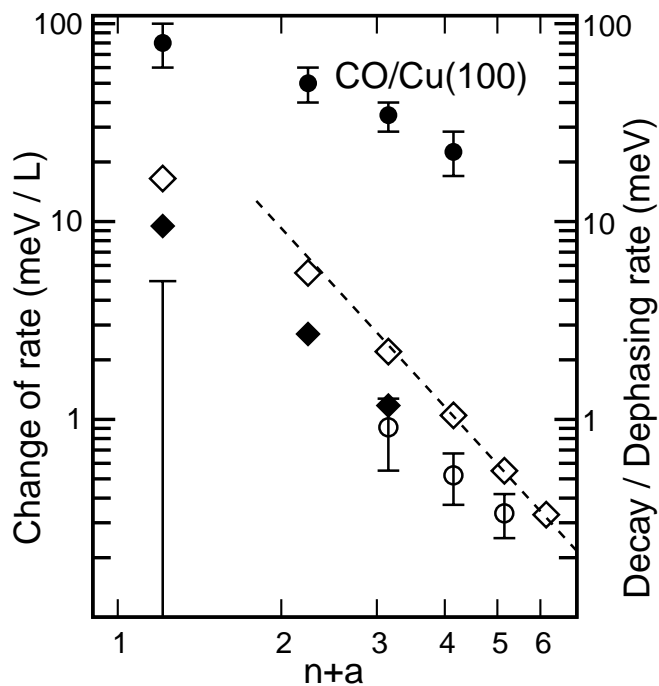


FIG. 4. Decay rate (diamonds) and pure dephasing rates (circles) for image potential states up to  $n = 6$ . The open symbols show the data for the clean Cu(100) surface and the filled symbols the initial slope for low CO exposures. For the decay rates the error bars are comparable to the symbol size. For the pure dephasing rate of the  $n = 1$  state only an upper limit is indicated. The quantum defect  $a$  takes the observed binding energy of the image-potential states into account [3,12].

quantum beats (see Fig. 2). The combination of the lifetime of  $40 \pm 6$  fs [12] and the linewidth of  $15 \pm 5$  meV (see Fig. 3) gives an upper limit of 5 meV (indicated by the error bar in Fig. 4) for the pure dephasing rate of the  $n = 1$  image-potential state. The decay rate shows a  $n^{-3}$  dependence for  $n \geq 3$  (dashed line in Fig. 4) as predicted by theory [8] and a slightly smaller slope for lower  $n$ . The pure dephasing rate on the clean surface is a factor of  $\sim 2$  smaller and shows a weaker dependence on  $n$  than the decay rate. The pure dephasing on the clean surface can be attributed to electron-phonon scattering [7,14] and to residual defects [15].

The decay and pure dephasing rates are found to increase linearly with CO exposures for coverages below 0.1 ML (see dashed lines in Fig. 3 for the  $n = 1$  state). The  $n$  dependence of these slopes is shown by filled symbols in Fig. 4. The change of the pure dephasing rate with CO exposure is about 1 order of magnitude larger than the change of the decay rate. This is consistent with the previous statement that the elastic scattering processes due to disordered adsorbate atoms have a strong influence on the pure dephasing rate and affect the decay rate less.

The changes upon CO exposure of the decay rate as well as the pure dephasing rate parallel the  $n$  dependence of the corresponding quantities found on the clean surface. This indicates that similar decay and dephasing mechanisms are at work for the clean and CO-covered surfaces. In the phase analysis picture [8] and its classical counterpart for large quantum numbers [4] the electron is reflected back and forth between the surface and the vacuum barrier. Decay is possible only into bulk states and, therefore, occurs mainly at the surface. This picture gives the asymptotic  $n^{-3}$  dependence for the decay rate cited above [8]. If the CO molecules open decay channels proportional to the exposure, the change of the decay rate with exposure would show the same behavior as a function of  $n$  as the decay rate found for the clean surface in agreement with the experimental findings in Fig. 4.

Under the reasonable assumption that the quasielastic scattering processes due to the imperfect CO overlayer occur only at the surface, one would expect the same  $n$  dependence for the pure dephasing rate as for the decay rate. This is in contrast to the experimental results (filled circles in Fig. 4) which show a significantly weaker dependence. The energy differences between the different image-potential states in the series are quite small so that an energy-dependent scattering cross section seems an unlikely explanation. Taking  $k_{\parallel}$  dependent scattering mechanisms into account the dephasing rates are proportional to the inverse of the effective mass [15]. The effective mass of the  $n = 1$  image-potential state on Cu(100) [3] is equal to the free-electron mass and the same is expected for the higher states [8]. Therefore, no effect depending on  $n$  arises from this mechanism.

Two effects might offer an explanation for the weak  $n$  dependence of the dephasing rate: (i) the lateral range an

electron in front of the surface samples is of the order of the distance from the surface as known from the concept of the local work function [16]. Therefore, an electron with low quantum number  $n$  has a higher probability to find a well-ordered patch on the surface and consequently a lower dephasing rate. (ii) For higher image-potential states the electrons need considerable time from the point of excitation at the surface to reach the classical turning point [4]. Scattering by the defects at the surface is particularly effective during the first part of the trajectory and might explain why the dephasing rate is higher for large  $n$  compared to the expected  $n^{-3}$  dependence.

In summary, we have identified the main contribution to the dephasing rate as quasielastic scattering processes which can be correlated with and controlled by the order of adsorbate overlayers. This is an important aspect for the electron dynamics in such systems and photon or electron-induced chemical reactions at surfaces. Further work on other adsorbates and towards a quantitative theoretical description is needed.

We thank W. Wallauer for help in the early stages of the experiments. Support by the Deutsche Forschungsgemeinschaft is gratefully acknowledged.

- 
- [1] C. Keller *et al.*, Phys. Rev. Lett. **80**, 1774 (1998); N.-H. Ge *et al.*, Science **279**, 202 (1998); E. W. Plummer, Science **277**, 1447 (1997); A. Hotzel *et al.*, Chem. Phys. Lett. **285**, 271 (1998).
  - [2] H. Petek and S. Ogawa, Prog. Surf. Sci. **56**, 239 (1997).
  - [3] Th. Fauster and W. Steinmann in *Photonic Probes of Surfaces*, Electromagnetic Waves: Recent Developments in Research, Vol. 2, edited by P. Halevi (North-Holland, Amsterdam, 1995), Chap. 8, p. 347.
  - [4] U. Höfer *et al.*, Science **277**, 1480 (1997).
  - [5] T. Hertel *et al.*, Vac. Sci. Technol. A **15**, 1503 (1997).
  - [6] M. Wolf, A. Hotzel, E. Knoesel, and D. Velic, Phys. Rev. B (to be published).
  - [7] E. Knoesel, A. Hotzel, and M. Wolf, J. Electron Spectrosc. Relat. Phenom. **88-91**, 577 (1998).
  - [8] P. M. Echenique and J. B. Pendry, Prog. Surf. Sci. **32**, 111 (1990).
  - [9] E. V. Chulkov *et al.*, Phys. Rev. Lett. **80**, 4947 (1998).
  - [10] J. Rogozik *et al.*, Phys. Rev. B **32**, 4296 (1985); K.-D. Tsuei and P. D. Johnson, Phys. Rev. B **45**, 13 827 (1992).
  - [11] K. Heinz, Rep. Progr. Phys. **58**, 637 (1995).
  - [12] I. L. Shumay *et al.*, Phys. Rev. B **58**, 13 974 (1998).
  - [13] S. Schuppler, N. Fischer, Th. Fauster, and W. Steinmann, Phys. Rev. B **46**, 13 539 (1992); **47**, 10 058(E) (1993).
  - [14] R. Matzdorf, G. Meister, and A. Goldmann, Surf. Sci. **286**, 56 (1993).
  - [15] F. Theilmann, R. Matzdorf, G. Meister, and A. Goldmann, Phys. Rev. B **56**, 3632 (1997).
  - [16] K. Wandelt, in *Thin Metal Films and Gas Chemisorption*, edited by P. Wissmann, Studies in Surface Science and Catalysis (Elsevier, Amsterdam, 1987) p. 280; R. Fischer *et al.*, Phys. Rev. Lett. **70**, 654 (1993).